Stem Cell Reports
Article

ISSCR

OPEN ACCESS

Aberrant nucleosome organization in mouse SCNT embryos revealed by ULI-MNase-seq

Lingyue Yang,[1,2,3] Xiaocui Xu,[1,2,3] Ruimin Xu,[2] Chuan Chen,[1] Xiaolei Zhang,[2] Mo Chen,[1] Xiaochen Kou,[1] Yanhong Zhao,[1] Hong Wang,[1] Xiaoyu Liu,[2,*] Shaorong Gao,[1,2,*] and Chong Li[1,*]

[1]Clinical and Translation Research Center of Shanghai First Maternity & Infant Hospital, Shanghai Key Laboratory of Signaling and Disease Research, Frontier Science Center for Stem Cell Research, School of Life Sciences and Technology, Tongji University, Shanghai 200092, China
[2]Institute for Regenerative Medicine, Shanghai East Hospital, Shanghai Key Laboratory of Signaling and Disease Research, Frontier Science Center for Stem Cell Research, School of Life Sciences and Technology, Tongji University, Shanghai 200120, China
[3]These authors contributed equally
*Correspondence: liuxiaoyu@tongji.edu.cn (X.L.), gaoshaorong@tongji.edu.cn (S.G.), lichong@tongji.edu.cn (C.L.)
https://doi.org/10.1016/j.stemcr.2022.05.020

SUMMARY

Somatic cell nuclear transfer (SCNT) can reprogram terminally differentiated somatic cells into totipotent embryos, but with multiple defects. The nucleosome positioning, as an important epigenetic regulator for gene expression, is largely unexplored during SCNT embryonic development. Here, we mapped genome-wide nucleosome profiles in mouse SCNT embryos using ultra-low-input MNase-seq (ULI-MNase-seq). We found that the nucleosome-depleted regions (NDRs) around promoters underwent dramatic reestablishment, which is consistent with the cell cycle. Dynamics of nucleosome position in SCNT embryos were delayed compared to fertilized embryos. Subsequently, we found that the aberrant gene expression levels in inner cell mass (ICM) were positively correlated with promoter NDRs in donor cells, which indicated that the memory of nucleosome occupancy in donor cells was a potential barrier for SCNT-mediated reprogramming. We further confirmed that the histone acetylation level of donor cells was associated with the memory of promoter NDRs. Our study provides insight into nucleosome reconfiguration during SCNT preimplantation embryonic development.

INTRODUCTION

Terminally differentiated somatic cells can be reprogrammed into totipotent embryos, thereby generating an entire organism through the somatic cell nuclear transfer (SCNT) technique, which is also called cloning (Gurdon, 1962; Wakayama et al., 1998; Wilmut et al., 1997). Since the birth of the first cloned mammal, Dolly the sheep, in 1997 (Wilmut et al., 1997), more than 20 mammalian species have been cloned successfully (Matoba and Zhang, 2018). In addition, the SCNT technique can be used to generate nuclear transfer-derived embryonic stem cells (ntESCs) that are similar to embryonic stem cells (ESCs) (Brambrink et al., 2006; Wakayama et al., 2001), and human senescent or patient-specific ntESCs have been successfully derived and have potential trends in clinical applications (Chung et al., 2014, 2015; Tachibana et al., 2013; Yamada et al., 2014). Therefore, the SCNT technique is expected to be advantageous for the preservation of endangered animals and the treatment of human diseases (Matoba and Zhang, 2018; Wakayama et al., 2008; Yang et al., 2007).

The SCNT technique also has many defects, however. The birth rate of cloned embryos is much lower than that of fertilized embryos (Matoba and Zhang, 2018). Moreover, cloned offspring often have abnormalities, such as a hypertrophic placenta (Ogura et al., 2013). Previous studies have shown that the development of cloned embryos is impeded by several epigenetic barriers, including aberrant imprinting gene *Xist* activation (Inoue et al., 2010; Matoba et al., 2011) and abnormal DNA methylation (Gao et al., 2018) and histone modifications (Inoue et al., 2020; Liu et al., 2016a; Matoba et al., 2014; Wang et al., 2020; Yang et al., 2021). Although treatment with histone deacetylase inhibitors (Kishigami et al., 2006; Van Thuan et al., 2009), deletion of *Xist* on the active X chromosome (Inoue et al., 2010; Matoba et al., 2011), overexpression of the histone demethylases *Kdm4b/4d/5b* (Liu et al., 2016a; Matoba et al., 2014), inhibition of DNA methyltransferase (Dnmts) (Gao et al., 2018), and overexpression of *Dux* (Yang et al., 2020, 2021) can significantly improve the developmental rate of cloned embryos, the birth defects of cloned embryos are not completely ameliorated (Matoba and Zhang, 2018). This suggests that there are other unknown barriers that need to be explored in SCNT embryos.

The nucleosomes are composed of histone octamers and wrapped genomic DNA, which are the basic units of chromatin in eukaryotes (Luger et al., 1997; Richmond and Davey, 2003; Tessarz and Kouzarides, 2014). The nucleosomes are connected by linker DNA to form a "beads-on-a-string" structure (Kornberg, 1974; Kujirai and Kurumizaka, 2020; Olins and Olins, 1974). At promoters, enhancers and transcription factor (TF) binding sites, nucleosome-depleted regions (NDRs), which are suitable for TF binding, are usually observed (Bernstein et al., 2004; Chereji and Clark, 2018; Lee et al., 2004; Sekinger et al., 2005). Furthermore, the canonical nucleosome pattern, which includes obvious NDRs, precisely positioned +1 and −1 nucleosomes, is

present at most activated promoters (Jiang and Pugh, 2009; Segal et al., 2006). Previous studies have shown that the nucleosome arrangement is closely related to transcriptional regulation (Kujirai and Kurumizaka, 2020; Nocetti and Whitehouse, 2016; Ramachandran and Henikoff, 2016; Zhu et al., 2018), and the canonical nucleosome pattern forms at promoters during zygotic genome activation (ZGA) (Zhang et al., 2014), which suggests that the dynamics of nucleosome arrangement are an important process for cell fate transition and somatic cell reprogramming.

Nucleosome remodeling occurs quickly after fertilization, which is necessary for embryonic development (Oliva, 2006; Wang et al., 2022). This process also occurs during SCNT embryonic development (Tao et al., 2017; Wen et al., 2014), but how the nucleosome position changes after the donor cell nucleus is transferred into enucleated oocytes and the underlying mechanism is largely unexplored. Here, we performed genome-wide profiling of nucleosome occupancy and positioning in early mouse SCNT embryos using ultra-low-input micrococcal nuclease digestion-based high-throughput sequencing (ULI-MNase-seq) method. We compared the dynamics of the nucleosome arrangement between SCNT and fertilized embryos and found that the resistant nucleosome pattern in donor cells results in abnormal gene expression in SCNT embryos. We demonstrated that histone acetylation is related to the regulation of nucleosome rearrangement at promoter regions. Our study provides insight into nucleosome reconfiguration during the early development of SCNT embryos.

RESULTS

Rapid reprogramming of nucleosome positioning following SCNT

The dynamics of genome-wide nucleosome occupancy and positioning in mouse SCNT embryos remain unclear. To explore the initial timing of nucleosome reestablishment after the injection of somatic cell nuclei into enucleated oocytes, we injected H2B-RFP mRNA into reconstructed oocytes to visualize histone replacement dynamics every 5 min within 1 h after somatic cell nuclei injection (post-injected) (Figures S1A and S1B). We observed a weak H2B-RFP signal in the injected nucleus as early as 5 min post-injection (5 mpi), and it subsequently became more obvious (Figure S1B). This result was similar to that reported previously, in which *de novo* synthesized maternal H3.3 replaces donor nucleus-derived H3 after SCNT (Wen et al., 2014). These results indicate that nucleosome remodeling is a genome-wide event during SCNT-mediated reprogramming.

To further study the dynamics of nucleosome reconfiguration in SCNT embryos and explore the underlying molecular mechanisms, we performed ULI-MNase-seq using mouse SCNT embryos. We collected reconstructed embryos at different stages, including 0.5 h post-injection (hpi), 1 hpi (also known as 0 h post-activation, [hpa]), 0.5 hpa, 1 hpa, 1.5 hpa, 2 hpa, 3 hpa, 4 hpa, 6 hpa, 12 hpa, early-2-cell, late-2-cell, 4-cell, 8-cell, morula, as well as inner cell mass (ICM) and trophectoderm (TE) from blastocyst (Figure 1A). We also collected mouse cumulus cells (CCs), which were used as the donor cells for SCNT (Figure 1A). We evaluated the data quality of ULI-MNase-seq and ascertained that our replicate data were highly reproducible (Figures S1C–S1E). The lengths of the mapped reads were mainly enriched at approximately 147 bp, which is the DNA size in mononucleosomes (Figure S1D). After fertilization, the nucleosome occupancy of the paternal genome undergoes a dramatic increase, while this rapid *de novo* establishment process does not occur in the maternal genome (Wang et al., 2022). Similar to female pronuclei (PN) in fertilized embryos, the nucleosome occupation rate showed little change, and the enrichment of nucleosomes on different genomic elements was also relatively stable during SCNT embryonic development (Figures S1F and S1G).

We then calculated the nucleosome occupancy and positioning around transcription start sites (TSSs) of all genes. Intriguingly, nucleosome positioning around TSSs underwent dramatic dynamics during early mouse SCNT embryonic development. We found that the NDRs and precisely positioned +1 and −1 nucleosomes around TSSs disappeared as early as 1 hpi and were rebuilt until 6 h after activation of the SCNT embryos (Figure 1B). However, the NDR pattern around TSSs appears much earlier in fertilized embryos, with male PN at 1.5 h post-fertilization (hpf) and female PN at 3 hpf (Wang et al., 2022). Previous studies have shown that nucleosome arrangement is associated with the cell cycle, with fuzzier organization during S and M phases (Deniz et al., 2016). We hypothesized that the dynamics of nucleosome reconfiguration were also related to the cell cycle. This finding was further confirmed by mapping the nucleosome profiles around CCCTC-binding factor (CTCF) motifs, which showed that the NDRs at the center of CTCF motifs were removed at 1 hpi and reformed strong NDRs and well-positioned nucleosome arrays at 6 hpa (Figure S1H). These results are consistent with our previous research, which found that the metaphase-like chromatin state formed at 1 hpi and exited until 6 hpa in SCNT embryos (Chen et al., 2020). This cell-cycle-related nucleosome rearrangement promotes the reprogramming of the somatic cell chromatin state after injection into enucleated oocytes.

Differential dynamics of nucleosome reconfiguration between fertilized and SCNT embryos

To investigate whether nucleosome remodeling is associated with a low developmental rate of SCNT embryos, we compared the nucleosome profiles of mouse SCNT

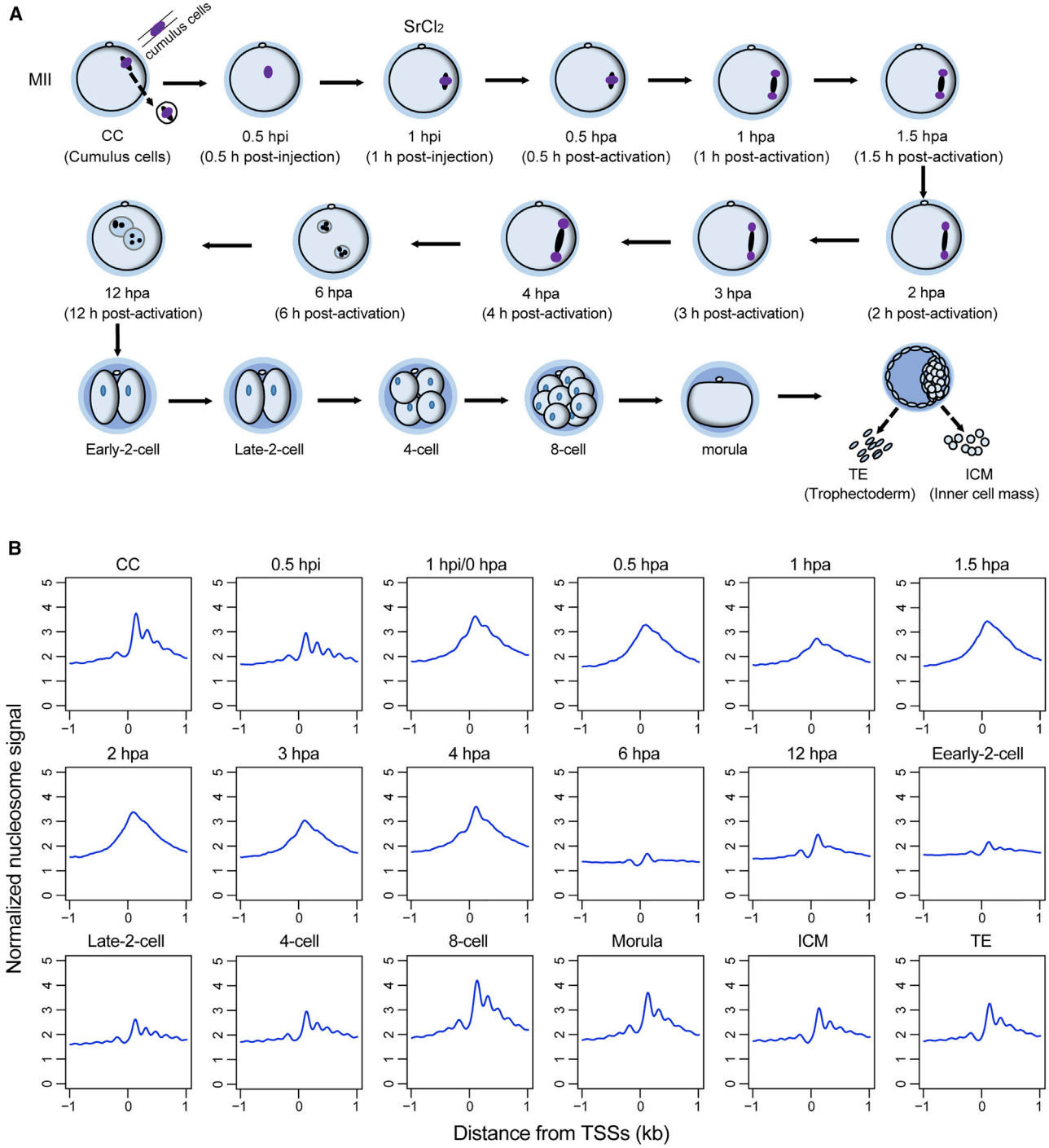

Figure 1. Rapid reprogramming of nucleosome occupancy and positioning in early SCNT embryonic development

(A) Schematic illustration of the SCNT procedure and sample collection for ULI-MNase-seq.

(B) Nucleosome profiles around TSSs of all genes in donor cells and each stage of SCNT embryos.

See also Figure S1 and Tables S1 and S2.

embryos with those of fertilized embryos in the corresponding stage. We compared the NDR scores at promoter regions (±2 kb around the TSSs) of all genes and found that the dynamics of nucleosome reconfiguration mapped by NDR scores were very different between fertilized and SCNT embryos (Figure 2A). The NDR scores in CCs were

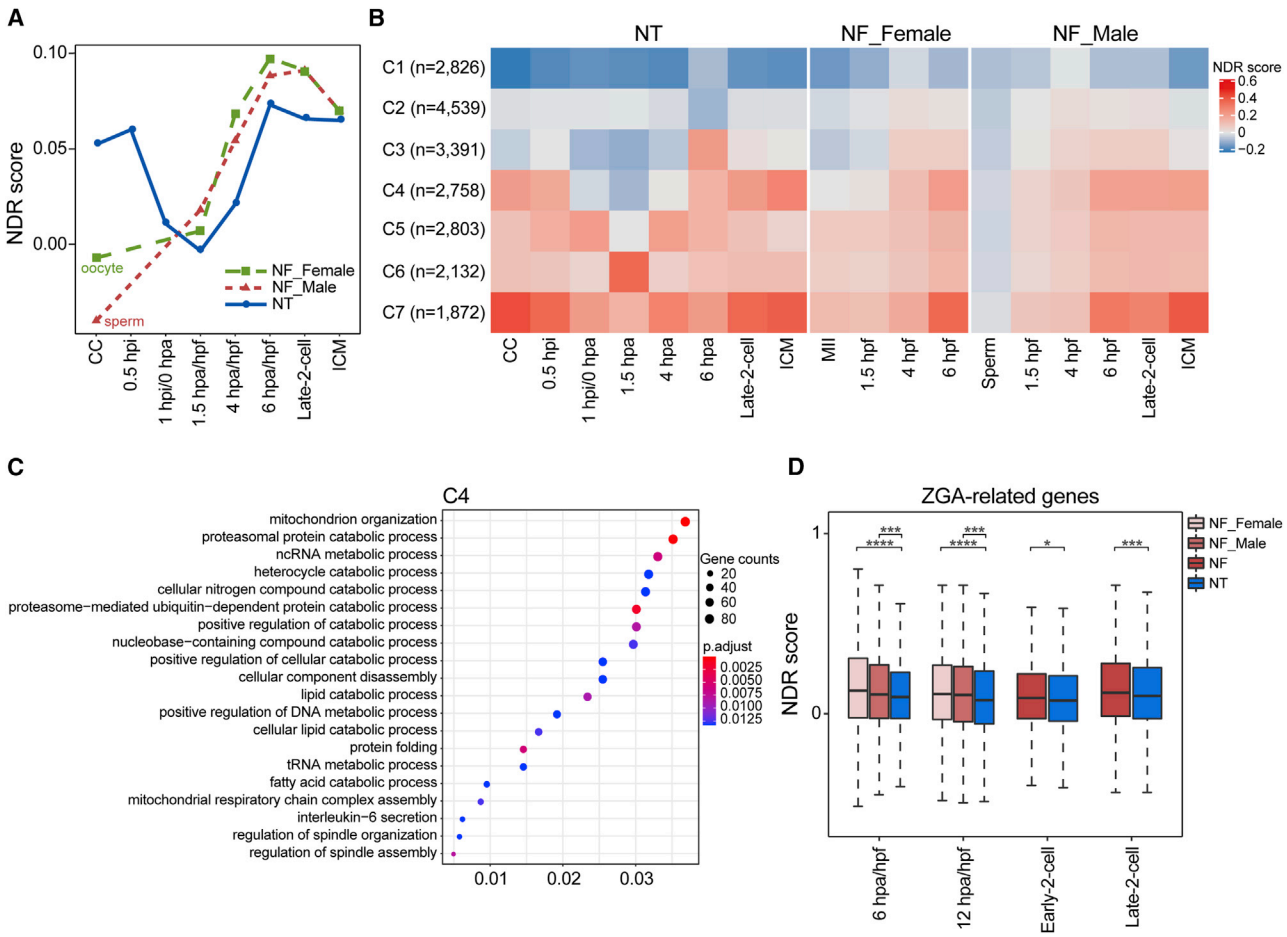

Figure 2. Differential dynamics of nucleosome remodeling between fertilized and SCNT embryos

(A) Graph showing the differential dynamics of NDR scores around TSSs of all genes between fertilized and SCNT embryos at each stage. NF, normal fertilization; NT, SCNT.

(B) Heatmap showing the k-means clustering (k = 7) of genes based on NDR scores around TSSs between fertilized and SCNT embryos at each stage.

(C) Gene Ontology analysis of cluster 4 classified in (B).

(D) Boxplot showing the NDRs around TSSs of ZGA genes based on NDR scores between fertilized and SCNT embryos at 6 hpa/hpf, 12 hpa/hpf, early-2-cell and late-2-cell stages (*p < 0.05; ***p < 0.001; ****p < 0.0001).

See also Figure S2 and Table S3.

much higher than those in sperm and oocytes; they showed an initial decrease followed by a subsequent increase in the SCNT embryos, while they generally continued to increase in the fertilized embryos (Figure 2A). We found that the NDR scores of SCNT embryos decreased to less than those of fertilized embryos at 1.5 hpa, and they remained lower than those of fertilized embryos, indicating that NDR reestablishment around TSSs occurred later in SCNT embryos than in fertilized embryos (Figure 2A). Finally, NDR scores in the ICM stage between SCNT and fertilized embryos were comparable (Figure 2A), which indicates more complete chromatin structure reprogramming in the blastocyst stage or that only properly reprogrammed embryos can develop to the blastocyst stage. These results suggest that the chromatin state of SCNT embryos needs to be reprogrammed to a state that is consistent with that of the fertilized embryos and then simulates the fertilized embryos for development.

To investigate the influence of nucleosome positioning defects on gene expression and SCNT embryonic development, we analyzed the difference in nucleosome remodeling between fertilized and SCNT embryos for each gene. We characterized all genes based on the NDR scores of promoters using k-means clustering, which revealed 7 clusters with differential NDR dynamics between fertilized and SCNT embryos (referred to as C1–C7; Figure 2B). The NDR

scores of genes in C1 were low in both fertilized and SCNT embryos; genes in C2 showed weaker NDRs in SCNT embryos starting from 4 hpa; genes in C3 showed significantly stronger NDRs in SCNT embryos at 6 hpa; NDRs of genes in C4 became weaker after 1 hpi in SCNT embryos and were then rebuilt at 6 hpa; NDRs of genes in C5, C6, and C7 were stable in both fertilized and SCNT embryos (Figure 2B). We next analyzed the expression level of the genes in each cluster in SCNT embryos and found that the gene expression level was generally positively correlated with the NDR scores (Figures S2A and S2B) (Wu et al., 2016).

To investigate whether the different NDR scores are related to the abnormal development of SCNT embryos, we performed Gene Ontology (GO) analysis for the genes in each cluster. The results showed that the genes in C4 were associated with the proteasomal protein catabolic process, ncRNA metabolic process, protein folding, regulation of spindle organization, and regulation of spindle assembly (Figure 2C). In addition, the genes in C1 and C2 were mainly associated with the regulation of body fluid levels or response to wounding, which are the function of somatic cells; the genes in C3, C5, and C6 were associated with the regulation of ion transmembrane transport and development of various organs, which are essential for postimplantation embryonic development; and C7′ genes were associated with DNA repair and nuclear division, which are essential for the fundamental activity of cells (Figures S2C–S2H).

ZGA after fertilization is very important for subsequent embryonic development, and similar events also occur in SCNT embryos. Previous studies have shown that ZGA is abnormal during SCNT embryonic development, and some genes are not successfully activated (Matoba and Zhang, 2018). We compared the NDR scores of ZGA-related genes around TSSs of fertilized and SCNT embryos at the 6 hpa, 12 hpa, early-2-cell, and late-2-cell stages. Interestingly, we found that the NDR scores of SCNT embryos were significantly lower than those of fertilized embryos (Figure 2D), implying that at the promoters of ZGA-related genes, TFs could not successfully access DNA because of the high nucleosome occupancy. These results indicate that incomplete ZGA may be related to the abnormal formation of NDRs at promoters in SCNT embryos.

Taken together, our results suggest that the nucleosome reconfiguration of SCNT embryos is obviously different from that of fertilized embryos, especially in the ZGA stage, which may be responsible for the low developmental rate of SCNT embryos.

Nucleosome positioning in donor cells is a potential barrier for the regulation of transcription during SCNT-mediated reprogramming

Since nucleosome remodeling plays an important role in the reprogramming of fertilized embryos, as well as in SCNT embryos, we next tried to explore the reasons for the abnormal nucleosome reconstruction in SCNT embryos, which led to the failure of reprogramming. We pairwise compared the transcriptome of donor cells, ICM in SCNT embryos, and ICM in fertilized embryos and identified 2,656 differentially expressed genes (DEGs) (fragments per kilobase of transcript per million mapped reads [FPKM] >5 in any sample, fold change >4 and false discovery rate [FDR] <0.05 were used as cutoff for DEGs) that may be related to the reprogramming process and classified these genes into four groups (Figures 3A and S3A). Of these DEGs, 823 genes were silenced in both SCNT and fertilized embryos (the relative expression level was high in donor cells and low in both SCNT and fertilized embryos [defined as HLL genes], n = 823). GO analysis revealed that they were mainly enriched in CC-specific biological processes such as regulation of angiogenesis and epithelial cell proliferation (Figures 3A and 3B). Although most of the highly expressed genes in donor cells were silenced in SCNT embryos, there was still a class of genes that failed to be repressed in SCNT embryos (the relative expression level was high in both donor cells and SCNT embryos but was low in fertilized embryos [defined as HHL genes], n = 397) (Figure 3A). HHL genes were associated with the development of reproductive organs, which need to be repressed in early embryonic development (Figure 3B). The majority of DEGs were activated in both SCNT and fertilized embryos (the relative expression level was low in donor cells and high in both SCNT and fertilized embryos [defined as LHH genes], n = 1,307), and these genes were significantly enriched in cell-cycle-related biological processes, such as DNA replication and chromosome segregation (Figures 3A and 3B). Compared to those in fertilized embryos, genes from the last group were not successfully activated in SCNT embryos (the relative expression level was low in both donor cells and SCNT embryos but was high in fertilized embryos [defined as LLH genes], n = 487), which possibly played important roles in embryonic development (Figures 3A and 3B).

Next, we examined the potential mechanism for the abnormal expression of HHL and LLH genes in SCNT embryos. We mapped the nucleosome profiles of the defined four groups of genes in SCNT embryos at each stage (Figure S3B). Interestingly, we found that the NDR scores of HHL genes were always higher than those of HLL genes, even in donor cells (Figures 3C and S3B), which indicates that the open chromatin state in donor cells may prevent the silencing of some somatic cell-specific genes. The NDR scores of LHH genes were also higher than those of LLH genes (Figures 3C and S3B), suggesting that the closed chromatin state also impedes the activation of embryo-specific genes. These results suggest that genes with more

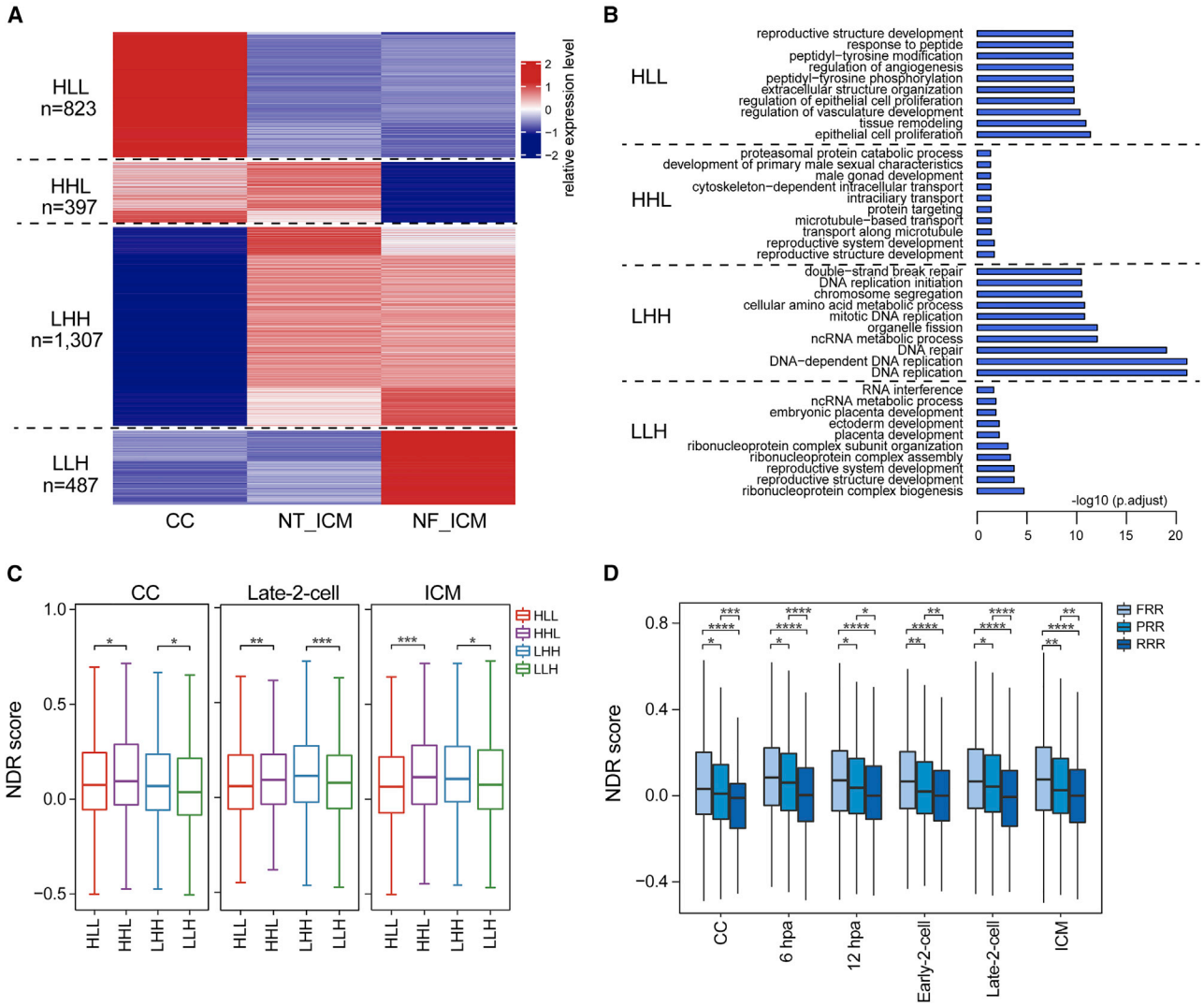

Figure 3. Aberrant nucleosome occupancy at promoters in donor cells causes incorrect reprogramming upon SCNT

(A) Heatmap showing the relative gene expression level for differentially expressed genes (DEGs) (fold change [FC] > 4, adjusted p value <0.05, FPKM >5 in at least one stage) obtained by a pairwise comparison between donor cells, SCNT ICM, and fertilized ICM embryos. A total of 2,656 DEGs were classified into 4 clusters by unsupervised hierarchical clustering. HLL, the relative expression level is high in donor cells and is low in both NT ICM and NF ICM embryos. HHL, the relative expression level is both high in donor cells and NT ICM embryos but is low in NF ICM embryos. LHH, the relative expression level is low in donor cells and is high in both NT ICM and NF ICM embryos. LLH, the relative expression level is both low in donor cells and NT ICM embryos but is high in NF ICM embryos.

(B) Gene Ontology analysis of the 4 groups classified in (A).

(C) Boxplot showing the NDRs around TSSs of 4 groups (A) of genes in donor cells, late-2-cell and ICM stage of SCNT embryos (*p < 0.05; **p < 0.01; ***p < 0.001).

(D) Boxplot showing the NDRs around TSSs of genes located at FRRs, PRRs, and RRRs based on NDR scores in donor cumulus cells and SCNT embryos at each stage. FRRs, PRRs, and RRRs indicate fully reprogrammed regions, partially reprogrammed regions, and reprogramming resistant regions, respectively (defined by Matoba et al., 2014) (*p < 0.05; **p < 0.01; ***p < 0.001; ****p < 0.0001).

See also Figure S3 and Table S4.

pronounced NDRs at promoters in donor cells were more likely to be activated during the development of SCNT embryos.

Reprogramming resistant regions (RRRs), which cannot be expressed normally in 2-cell SCNT embryos, impeded the development of SCNT embryos and were mainly

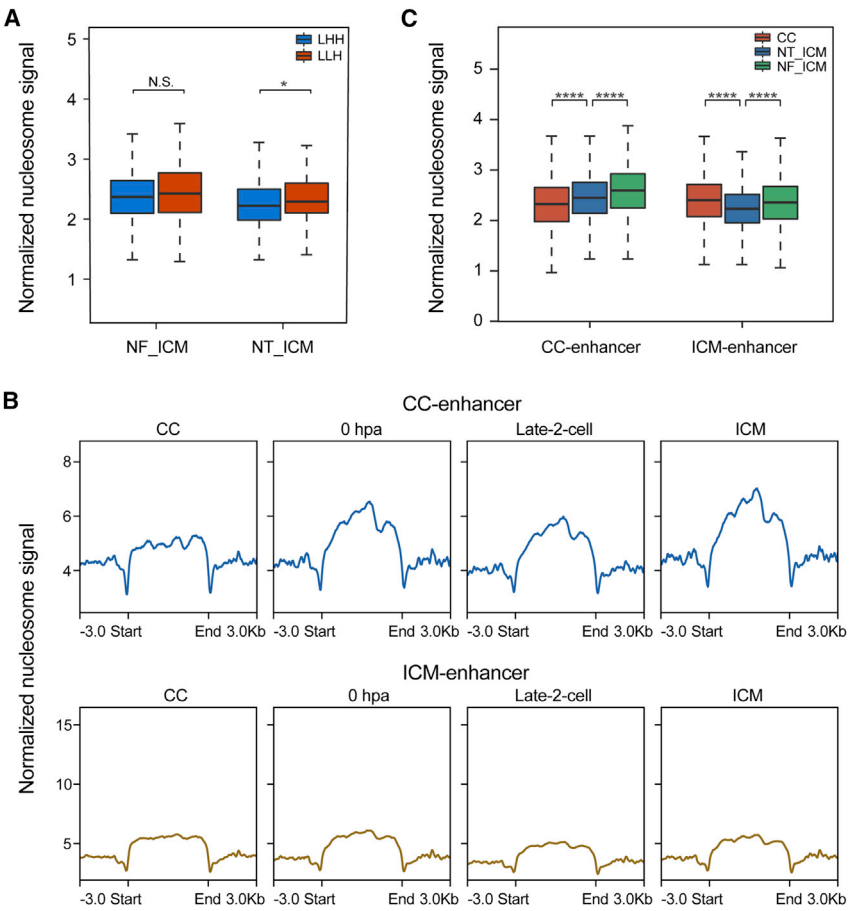

Figure 4. Incorrect nucleosome occupancy at enhancers is a factor in abnormal gene expression

(A) Boxplot showing the nucleosome occupancy at ICM-specific enhancers of LHH and LLH genes classified in Figure 3A between fertilized and SCNT embryos in the ICM stage (*$p < 0.05$).

(B) Nucleosome profiles at CC enhancers (above) and ICM enhancers (below) of all genes at each stage sample.

(C) Boxplot showing the nucleosome occupancy at CC enhancers and ICM enhancers of CC, ICM SCNT, and ICM fertilized embryos (****$p < 0.0001$).

See also Figure S4 and Table S2.

enriched for H3K9me3 in donor cells (Matoba et al., 2014). To test our results further, we mapped the nucleosome profiles of promoters located at fully reprogrammed regions (FRRs), partially reprogrammed regions (PRRs) and RRRs and calculated the NDR scores for them. Consistent with our previous results, FRRs had the highest NDR scores in all stages, while RRRs had almost no NDRs, and PRR values were in the middle (Figures 3D and S3C). These results further confirmed that genes with more obvious NDRs in donor cells were more easily activated during the ZGA process.

Taken together, these results suggest that nucleosome occupancy at promoters is comparatively stable during SCNT-mediated reprogramming and that stable nucleosome position is a potential epigenetic barrier for gene activation or silencing.

Nucleosome occupancy at enhancers affects gene expression

In addition to promoters, enhancers play an important role in regulating gene expression. To study whether the aberrant nucleosome occupancy at enhancers results in abnormal gene expression in SCNT embryos, we identified CC, late-2-cell, and ICM enhancers by H3K4me1 and H3K27ac peaks in fertilized embryos (Figures S4A and S4B). Combined with the nucleosome profiles, these data showed that the nucleosome occupancy at ICM enhancers of LLH genes was significantly higher than that of LHH genes in the ICM stage of SCNT embryos instead of fertilized embryos (Figures 4A, S4C, and S4D), which implied that high nucleosome occupancy in enhancer regions was also involved in the aberrant gene expression in SCNT embryos. However, we did not observe similar results at late-2-cell enhancers (Figure S4D), which may be due to the incomplete establishment of the enhancers at this stage (Wu et al., 2016). To investigate the nucleosome positioning dynamics in enhancer regions, we mapped the nucleosome profiles of CC enhancers and ICM enhancers in donor cells and the 0 hpa, late-2-cell, and ICM stages of SCNT embryos and found that nucleosome occupancy at CC enhancers was rebuilt at later developmental stages of SCNT embryos but was still lower than that at the ICM of fertilized embryos, which indicated that the silenced state of CC enhancers was not completely reestablished

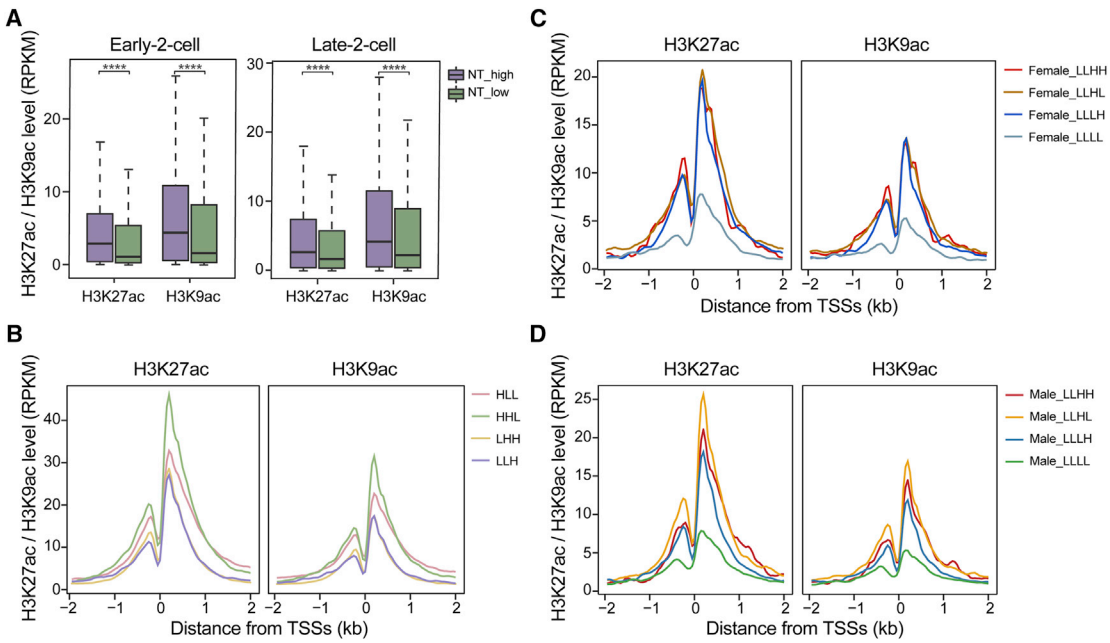

Figure 5. Histone acetylation is associated with nucleosome establishment in mouse SCNT embryos

(A) Boxplot showing the H3K27ac and H3K9ac levels of donor cells for promoters of genes in the early-2-cell-differential (left) (classified in Figure S5A) and late-2-cell-differential NDR clusters (right) (classified in Figure S5B) (****$p < 0.0001$).

(B) Graph showing the H3K27ac (left) and H3K9ac (right) levels on the promoters of genes in the 4 groups classified in Figure 3A in donor cells.

(C) Graph showing the H3K27ac (left) and H3K9ac (right) levels in the promoters of genes in different promoter NDR clusters (classified in Figure S5C) in donor cells.

(D) Graph showing the H3K27ac (left) and H3K9ac (right) levels in the promoters of genes in different promoter NDR clusters (classified in Figure S5D) in donor cells.

See also Figure S5 and Table S5.

in SCNT embryos (Figures 4B and 4C). However, nucleosome occupancy at ICM enhancers was reduced to a level that was even lower than that in the ICM of fertilized embryos during SCNT embryonic development, which suggests a more open chromatin state in these enhancer regions in SCNT embryos (Figures 4B and 4C). These results suggest that nucleosome occupancy at enhancer regions is more dynamic but also results in abnormal gene expression in SCNT embryos.

Histone acetylation correlates with nucleosome repositioning in SCNT embryos

Next, we investigated the potential factors that affect nucleosome repositioning during the reprogramming of SCNT embryos. Our recent study has shown that histone acetylation influences the establishment of NDRs in male PN after fertilization (Wang et al., 2022). Therefore, we defined NT-specific high NDR genes (NT-high) and NT-specific low NDR genes (NT-low) by comparing the NDR scores of promoters between SCNT and fertilized embryos at the early-2-cell or late-2-cell stage (Figures S5A and S5B). We compared the levels of H3K9ac and H3K27ac of these genes in donor cells and found that the level of histone acetylation was extremely high in the NT-high gene promoters defined by both early-2-cell and late-2-cell embryos (Figure 5A). These results suggest that histone acetylation in donor cells is related to NDR reprogramming in SCNT embryos.

To further investigate the effect of histone acetylation on the dynamics of nucleosome positioning, we compared the levels of H3K9ac and H3K27ac in the four groups of DEGs (classified in Figure 3A) in donor cells and found that the levels of H3K9ac and H3K27ac in HHL genes, which demonstrated higher NDR scores, were significantly higher than those of HLL genes (Figure 5B), indicating that the formation of a closed chromatin state of these genes may be hampered by enriched histone acetylation in donor cells. Instead, the levels of H3K9ac and H3K27ac between LHH and LLH genes exhibited no significant difference in donor cells (Figure 5B), which may be because the influence weakened in blastocyst stage or other epigenetic modifications are involved in the regulation of these genes.

To further confirm our conjecture, we classified selected genes with low promoter NDR scores at 6 hpa/hpf in both SCNT and fertilized embryos, which revealed 4 clusters with differential NDR dynamics at 12 hpa/hpf between SCNT and fertilized embryos (Figures S5C–S5F). For the 4 clusters (called LLHH/LLLH/LLHL/LLLL genes, respectively), here, "L" indicated that the NDR scores around TSSs were low and "H" indicated that the NDR scores around TSSs were high. The four letters each represented the NDR scores at 6 hpa of SCNT embryos, 6 hpf of fertilized embryos, 12 hpa of SCNT embryos, and 12 hpf of fertilized embryos (Figures S5C and S5D). We found that genes with higher levels of H3K27ac and H3K9ac in donor cells tended to reestablish stronger NDRs at 12 hpa/hpf (Figures 5C, 5D, S5G, and S5H). In addition, we observed the H3K27ac, H3K9ac, and H3K9me3 levels in the 7 clusters of genes (classified in Figure 2B) in donor cells and consistently found that histone acetylation was closely related to promoter NDRs in SCNT embryos (Figure S5I). Taken together, these results suggest that histone acetylation is related to nucleosome repositioning during the reprogramming of SCNT embryos.

DISCUSSION

Although some epigenetic barriers have been explored in SCNT embryos and cloning efficiency has been improved to a certain extent, the birth rate of cloned embryos is much lower than that of fertilized embryos (Chen et al., 2020; Gao et al., 2018; Inoue et al., 2010; Liu et al., 2016a; Matoba et al., 2014; Matoba and Zhang, 2018; Yang et al., 2021). During the reprogramming of SCNT embryos, it is not clear how nucleosome remodeling occurs and whether there is a difference compared with fertilized embryos. In this study, we mapped genome-wide nucleosome profiles during early mouse SCNT embryonic development. We found that the nucleosome remodeling of SCNT embryos is different from that of fertilized embryos. In addition, we investigated the possible causes of aberrant nucleosome occupancy reprogramming in SCNT embryos and found that histone acetylation was associated with nucleosome repositioning in SCNT embryos.

Because the effects of MNase-associated bias on the determination of nucleosome positioning are still debated (Allan et al., 2012; Chung et al., 2010), the data are strongly affected by the efficiency of MNase digestion. We established multiple duplicates in each stage and normalized the ULI-MNase-seq data by bioinformatics analysis to minimize the impact. When comparing different samples by calculating the promoter NDR scores, we found that the nucleosomes were rearranged rapidly after the donor cells were injected into the enucleated oocytes, with the typical NDRs of promoters disappearing at 1 hpi and continually rebuilt until 6 hpa in SCNT embryos (Figure 1B). In addition, when comparing the SCNT and fertilized embryos based on the promoter NDR scores, we found that the nucleosome arrangement of donor cells seemed to return to a state similar to that of MII oocytes, which are in the metaphase stage, and then simulated the process of nucleosome remodeling in fertilized embryos (Figure 2A).

The cytoplasm of oocytes can reprogram the chromatin of sperm, with the protamine replaced by histones rapidly after fertilization (Wang et al., 2022). Histone replacement also occurs in SCNT embryos (Wen et al., 2014), which may promote the rapid nucleosome position changes. This process may rely on the function of some maternal factors such as ATP-dependent chromatin remodelers in the cytoplasm of oocytes (Konev et al., 2007). Furthermore, the rapid remodeling was also found during the reprogramming of 3D chromatin structure in SCNT embryos, and the 3D chromatin structure of donor cells can be converted to the metaphase-like state within 1 h after nuclear transfer (Chen et al., 2020). The change of cell-cycle phase may be an inducer of the chromatin remodeling. Whether loss of function of these cell-cycle-related factors in oocyte cytoplasm can disturb the rapid nucleosome position reprogramming deserves further investigation.

Considering the resolution limits of ULI-MNase-seq, it is difficult to map the nucleosome profiles of a single gene, so we defined different gene groups for analysis. Silent genes often show high nucleosome occupancy at promoters, and strong promoter NDRs are usually linked to gene activation (Levitsky et al., 2020; Tao et al., 2014; Zhang et al., 2014). Our recent study showed abnormal H3K9ac in SCNT embryos resulting in reduced 2-cell genome activation (Yang et al., 2021). Our analysis suggested that the aberrant high nucleosome occupancy at promoters in donor cells impeded the activation of corresponding genes in SCNT embryos, and the nucleosome repositioning of this part of the genes was possibly regulated by histone acetylation, of which the genes with high histone acetylation levels in promoters tend to form stronger NDRs and be activated. However, the genes that had lower nucleosome occupancy at promoters, which were more open chromatin, may be mainly affected by other epigenetic modifications to direct nucleosome repositioning and make its chromatin close or remain open. The developmental rate of SCNT embryos may be improved by increasing the promoter histone acetylation level of the silent genes in the donor cells and pushing NDR formation normally during SCNT embryonic development. However, due to the wide range of effects of histone deacetylase inhibitors, there is no appropriate method to achieve this. ATP-dependent chromatin remodeling complexes are required for the formation of precise nucleosome-positioning patterns (Gkikopoulos et al., 2011; Konev et al., 2007; Tolstorukov et al., 2013), and knockdown or overexpression of these remodelers in donor cells may aid in the correction of aberrant nucleosome

patterns. More precise regulation can be achieved by the dCas9 system in conjunction with nucleosome remodeling complexes (e.g., SWI/SNF) to rescue specific regions of aberrant nucleosome occupancy. Pioneer factors are able to bind within condensed chromatin and establish permissive chromatin states for gene activation (Zaret and Carroll, 2011). A previous study has shown that promoter nucleosome organization before genome activation can predict future gene activation, which can be used to speculate potential pioneer factors or chromatin remodelers (Zhang et al., 2014). Overexpression of these pioneer factors that are aberrantly expressed in SCNT embryos may benefit the establishment of precise nucleosome-positioning patterns and improve SCNT efficiency. These may be interesting research topics in the future. Overall, our study provides insight into nucleosome reconfiguration during early SCNT embryonic development.

EXPERIMENTAL PROCEDURES

Animals and mouse embryo collection and somatic cell nuclear transfer

A detailed description is provided in the supplemental experimental procedures.

H2B-RFP overexpression followed by immunostaining in SCNT embryos, and sample harvest for ULI-MNase-seq and chromatin immunoprecipitation sequencing (ChIP-seq)

A detailed description is provided in the supplemental experimental procedures.

Isolation of PN in SCNT embryos

At 0.5 hpi, 1 hpi, and 0.5 hpa, 1 hpa, 1.5 hpa, 2 hpa, 3 hpa, and 4 hpa, the embryos were placed in HCZB medium containing Hoechst 33342 dye to visualize the PN. At 6 hpa and 12 hpa, the PN were visible and did not need to be stained. The PN were isolated by a Piezo-drill micromanipulator puncturing zona pellucidae. Isolated PN were washed thoroughly in 0.5% BSA-PBS to avoid contamination and then placed in lysis buffer for ULI-MNase-seq.

ULI-MNase-seq

The ULI-MNase libraries were generated according to a previous protocol (Wang et al., 2022). A detailed description is provided in the supplemental experimental procedures.

ULI-NChIP-seq

The ULI-NChIP procedure was performed as previously described (Liu et al., 2016b). A detailed description is provided in the supplemental experimental procedures.

ULI-MNase-seq data processing

ULI-MNase-seq reads were aligned to the mouse genome build mm9 using the bwa (version 0.7.12) mem command. Reads with a mapping quality (MAPQ) less than 10 and duplicated reads were removed from downstream analyses. To create nucleosome profiles, we identified the centers of all paired-end reads and extended them to 146-bp lengths. To normalize the effect of sequencing depth, we scaled all of the nucleosome profiles to 500 million reads in total. To generate the length distribution plot, we randomly sampled 1 M paired-end reads of each sample. To examine the reproducibility of the MNase-seq libraries, we generated nucleosome profiles for all replicates and calculated the correlation of normalized nucleosome occupancy between biological replicates using promoter regions (defined as 2 kb upstream and downstream of TSSs) of Refseq genes. As the replicates were highly correlated with one another (Pearson's correlation >0.9), we pooled the biological replicates together for each stage. We generated the averaged nucleosome profiles around TSS regions using the plotprofile function from deepTools. For PCA, nucleosome signals of promoter regions were summarized by the bigWigAverageOverBed function from UCSC utilities. Then, the signals were subjected to the prcomp function in R, and the principal-component analysis (PCA) values were plotted by the ggplot2 package.

The NDR score was defined previously: NDR = (Max(+1, −1) − center)/(max(all) − min (all)), where +1 represents plus 1 nucleosome, which is the maximum of the normalized nucleosome profile from +50 to +250 bp of the TSS or motif center; −1 represents minus 1 nucleosome, which is the maximum of the normalized nucleosome profile from −250 to −50 bp of the TSS or motif center; the center region, which is defined as the mean of the normalized nucleosome profile from −50 to 50 bp; all represents all of the profiles, which represent −2 to +2 kb of the TSS or −1 to +1 kb of the motif center.

The enrichment of nucleosome regions on genomic elements, including promoters, exons, introns, long interspersed nuclear elements (LINEs), short interspersed nuclear elements (SINEs), and long terminal repeats (LTRs), was calculated using observed probability versus expected probability. The observed probability was calculated using the lengths of nucleosome regions that covered the designated genomic elements versus the lengths of total nucleosome regions, and the expected probability was calculated using the total lengths of designated genomic regions versus the length of the whole genome.

NDR clustering for differentially reprogrammed genes between NT and normal fertilization (NF) 12 hpa was conducted as follows. First, genes were restricted to those with NDR differences less than 0.1 between NT and NF 6 hpa. Second, NDR differences (between NT and NF 12 hpa) greater than 0.1 were defined as differentially reprogrammed; otherwise, they were defined as similar reprogrammed between NT and NF. Finally, differentially and similarly reprogrammed genes were further classified according to their NDR levels: NDR >0.1 was defined as "H," and NDR <0 was defined as "L." By applying the above criteria, we defined four classes: LLHH and LLLL represent similar reprogrammed genes, while LLHL and LLLH represent differentially reprogrammed genes.

Bulk RNA-seq data processing and ChIP-seq data analysis

A detailed description is provided in the supplemental experimental procedures.

Statistics and reproducibility

For all of the presented boxplots, the center represents the median value, and the lower and upper lines represent the 5% and 95% quantiles, respectively. Significant differences between different groups were determined using the Wilcoxon rank-sum test, and $p < 0.05$ was considered statistically significant. MNase-seq and ChIP-seq experiments were performed two to five times for each group, and the precise numbers of replicates are summarized in Table S1.

Data and code availability

The accession number for the sequencing data reported in this paper is GSA: CRA005944. These data have been deposited in the Genome Sequence Archive (Chen et al., 2021; CNCB-NGDC Members and Partners, 2022) under project PRJCA007996. The shared URL for review is https://ngdc.cncb.ac.cn/gsa/s/9nIdm06Y. All of the MNase-seq and ChIP-seq data generated in this study are summarized in Table S2. The MNase-seq data of fertilized embryos were downloaded from the GEO database (GSE140877) (Wang et al., 2022). RNA-seq data were downloaded from the GEO database (GSE66390 and GSE195760). All of the other data supporting the findings of this study are available from the corresponding author upon reasonable request.

SUPPLEMENTAL INFORMATION

Supplemental information can be found online at https://doi.org/10.1016/j.stemcr.2022.05.020.

AUTHOR CONTRIBUTIONS

C.L., X.L., and S.G. conceived the project and designed the experiments. L.Y. and C.L. performed most of the experiments, with the help of R.X., C.C., M.C., X.K., Y.Z., and H.W. X.X. performed most of the data analysis, with the help of L.Y. and X.Z. L.Y., X.X., X.L., C.L., and S.G. wrote the manuscript.

ACKNOWLEDGMENTS

We would like to thank Chenfei Wang from Tongji University and Yinyu Cui and Qianshu Zhu from the Cizhong Jiang laboratory for help with the bioinformatics analysis. We also thank Dr. K. Yamagata for providing the H2B-RFP plasmid. Furthermore, we are grateful to our laboratory colleagues for their assistance with experiments and advice. This work was supported by the National Key R&D Program of China (2020YFA0112500 and 2021YFA1102900) and the National Natural Science Foundation of China (31721003, 31820103009, 32070802, 32000418, and 32100645). This work was also supported by the Key Project of the Science and Technology of Shanghai Municipality (19JC1415300 and 21JC1405500), the China Postdoctoral Science Foundation (2021M692437 and 2020M681383), the Shanghai Rising-Star Program (20QA409700), the Shanghai Municipal Science and Technology Major Project (2021SHZDZX0100) and the Fundamental Research Funds for the Central Universities. The authors thank the Bioinformatics Supercomputer Center of Tongji University for offering computing resources.

CONFLICTS OF INTERESTS

The authors declare no competing interests.

Received: March 23, 2022
Revised: May 25, 2022
Accepted: May 26, 2022
Published: June 23, 2022

REFERENCES

Allan, J., Fraser, R.M., Owen-Hughes, T., and Keszenman-Pereyra, D. (2012). Micrococcal nuclease does not substantially bias nucleosome mapping. J. Mol. Biol. *417*, 152–164. https://doi.org/10.1016/j.jmb.2012.01.043.

Bernstein, B.E., Liu, C.L., Humphrey, E.L., Perlstein, E.O., and Schreiber, S.L. (2004). Global nucleosome occupancy in yeast. Genome Biol. *5*, R62. https://doi.org/10.1186/gb-2004-5-9-r62.

Brambrink, T., Hochedlinger, K., Bell, G., and Jaenisch, R. (2006). ES cells derived from cloned and fertilized blastocysts are transcriptionally and functionally indistinguishable. Proc. Natl. Acad. Sci. U S A *103*, 933–938.. https://doi.org/10.1073/pnas.0510485103.

Chen, M., Zhu, Q., Li, C., Kou, X., Zhao, Y., Li, Y., Xu, R., Yang, L., Yang, L., Gu, L., et al. (2020). Chromatin architecture reorganization in murine somatic cell nuclear transfer embryos. Nat. Commun. *11*, 1813. https://doi.org/10.1038/s41467-020-15607-z.

Chen, T., Chen, X., Zhang, S., Zhu, J., Tang, B., Wang, A., Dong, L., Zhang, Z., Yu, C., Sun, Y., et al. (2021). The genome sequence archive family: toward explosive data growth and diverse data types. Dev. Reprod. Biol. *19*, 578–583. https://doi.org/10.1016/j.gpb.2021.08.001.

Chereji, R.V., and Clark, D.J. (2018). Major determinants of nucleosome positioning. Biophys. J. *114*, 2279–2289. https://doi.org/10.1016/j.bpj.2018.03.015.

Chung, H.R., Dunkel, I., Heise, F., Linke, C., Krobitsch, S., Ehrenhofer-Murray, A.E., Sperling, S.R., and Vingron, M. (2010). The effect of micrococcal nuclease digestion on nucleosome positioning data. PLoS One *5*, e15754.. https://doi.org/10.1371/journal.pone.0015754.

Chung, Y.G., Eum, J.H., Lee, J.E., Shim, S.H., Sepilian, V., Hong, S.W., Lee, Y., Treff, N.R., Choi, Y.H., Kimbrel, E.A., et al. (2014). Human somatic cell nuclear transfer using adult cells. Cell Stem Cell *14*, 777–780.. https://doi.org/10.1016/j.stem.2014.03.015.

Chung, Y.G., Matoba, S., Liu, Y., Eum, J.H., Lu, F., Jiang, W., Lee, J.E., Sepilian, V., Cha, K.Y., Lee, D.R., and Zhang, Y. (2015). Histone demethylase expression enhances human somatic cell nuclear transfer efficiency and promotes derivation of pluripotent stem cells. Cell Stem Cell *17*, 758–766.. https://doi.org/10.1016/j.stem.2015.10.001.

Deniz, Ö., Flores, O., Aldea, M., Soler-López, M., and Orozco, M. (2016). Nucleosome architecture throughout the cell cycle. Sci. Rep. *6*, 19729. https://doi.org/10.1038/srep19729.

Gao, R., Wang, C., Gao, Y., Xiu, W., Chen, J., Kou, X., Zhao, Y., Liao, Y., Bai, D., Qiao, Z., et al. (2018). Inhibition of aberrant DNA Remethylation improves post-implantation development of somatic

cell nuclear transfer embryos. Cell Stem Cell *23*, 426–435.e5.. https://doi.org/10.1016/j.stem.2018.07.017.

Gkikopoulos, T., Schofield, P., Singh, V., Pinskaya, M., Mellor, J., Smolle, M., Workman, J.L., Barton, G.J., and Owen-Hughes, T. (2011). A role for Snf2-related nucleosome-spacing enzymes in genome-wide nucleosome organization. Science *333*, 1758–1760.. https://doi.org/10.1126/science.1206097.

Gurdon, J.B. (1962). The developmental capacity of nuclei taken from intestinal epithelium cells of feeding tadpoles. J. Embryol. Exp. Morphol. *10*, 622–640. https://doi.org/10.1242/dev.10.4.622.

Inoue, K., Kohda, T., Sugimoto, M., Sado, T., Ogonuki, N., Matoba, S., Shiura, H., Ikeda, R., Mochida, K., Fujii, T., et al. (2010). Impeding Xist expression from the active X chromosome improves mouse somatic cell nuclear transfer. Science *330*, 496–499.. https://doi.org/10.1126/science.1194174.

Inoue, K., Ogonuki, N., Kamimura, S., Inoue, H., Matoba, S., Hirose, M., Honda, A., Miura, K., Hada, M., Hasegawa, A., et al. (2020). Loss of H3K27me3 imprinting in the Sfmbt2 miRNA cluster causes enlargement of cloned mouse placentas. Nat. Commun. *11*, 2150. https://doi.org/10.1038/s41467-020-16044-8.

Jiang, C., and Pugh, B.F. (2009). A compiled and systematic reference map of nucleosome positions across the Saccharomyces cerevisiae genome. Genome Biol. *10*, R109. https://doi.org/10.1186/gb-2009-10-10-r109.

Kishigami, S., Mizutani, E., Ohta, H., Hikichi, T., Thuan, N.V., Wakayama, S., Bui, H.T., and Wakayama, T. (2006). Significant improvement of mouse cloning technique by treatment with trichostatin A after somatic nuclear transfer. Biochem. Biophys. Res. Commun. *340*, 183–189. https://doi.org/10.1016/j.bbrc.2005.11.164.

Konev, A.Y., Tribus, M., Park, S.Y., Podhraski, V., Lim, C.Y., Emelyanov, A.V., Vershilova, E., Pirrotta, V., Kadonaga, J.T., Lusser, A., and Fyodorov, D.V. (2007). CHD1 motor protein is required for deposition of histone variant H3.3 into chromatin in vivo. Science *317*, 1087–1090.. https://doi.org/10.1126/science.1145339.

Kornberg, R.D. (1974). Chromatin structure: a repeating unit of histones and DNA. Science *184*, 868–871.. https://doi.org/10.1126/science.184.4139.868.

Kujirai, T., and Kurumizaka, H. (2020). Transcription through the nucleosome. Curr. Opin. Struct. Biol. *61*, 42–49. https://doi.org/10.1016/j.sbi.2019.10.007.

Lee, C.K., Shibata, Y., Rao, B., Strahl, B.D., and Lieb, J.D. (2004). Evidence for nucleosome depletion at active regulatory regions genome-wide. Nat. Genet. *36*, 900–905. https://doi.org/10.1038/ng1400.

Levitsky, V.G., Zykova, T.Y., Moshkin, Y.M., and Zhimulev, I.F. (2020). Nucleosome positioning around transcription start site correlates with gene expression only for active chromatin state in Drosophila interphase chromosomes. Int. J. Mol. Sci. *21*, 9282. https://doi.org/10.3390/ijms21239282.

Liu, W., Liu, X., Wang, C., Gao, Y., Gao, R., Kou, X., Zhao, Y., Li, J., Wu, Y., Xiu, W., et al. (2016a). Identification of key factors conquering developmental arrest of somatic cell cloned embryos by combining embryo biopsy and single-cell sequencing. Cell Discov. *2*, 16010. https://doi.org/10.1038/celldisc.2016.10.

Liu, X., Wang, C., Liu, W., Li, J., Li, C., Kou, X., Chen, J., Zhao, Y., Gao, H., Wang, H., et al. (2016b). Distinct features of H3K4me3 and H3K27me3 chromatin domains in pre-implantation embryos. Nature *537*, 558–562.. https://doi.org/10.1038/nature19362.

Luger, K., Mäder, A.W., Richmond, R.K., Sargent, D.F., and Richmond, T.J. (1997). Crystal structure of the nucleosome core particle at 2.8 Å resolution. Nature *389*, 251–260.. https://doi.org/10.1038/38444.

Matoba, S., Inoue, K., Kohda, T., Sugimoto, M., Mizutani, E., Ogonuki, N., Nakamura, T., Abe, K., Nakano, T., Ishino, F., and Ogura, A. (2011). RNAi-mediated knockdown of Xist can rescue the impaired postimplantation development of cloned mouse embryos. Proc. Natl. Acad. Sci. U S A *108*, 20621–20626.. https://doi.org/10.1073/pnas.1112664108.

Matoba, S., Liu, Y., Lu, F., Iwabuchi, K.A., Shen, L., Inoue, A., and Zhang, Y. (2014). Embryonic development following somatic cell nuclear transfer impeded by persisting histone methylation. Cell *159*, 884–895.. https://doi.org/10.1016/j.cell.2014.09.055.

Matoba, S., and Zhang, Y. (2018). Somatic cell nuclear transfer reprogramming: mechanisms and applications. Cell Stem Cell *23*, 471–485.. https://doi.org/10.1016/j.stem.2018.06.018.

CNCB-NGDC Members and Partners (2022). Database resources of the national genomics data center, China national center for bioinformation in 2022. Nucleic Acids Res. *50*, D27–D38. https://doi.org/10.1093/nar/gkab951.

Nocetti, N., and Whitehouse, I. (2016). Nucleosome repositioning underlies dynamic gene expression. Genes Dev. *30*, 660–672. https://doi.org/10.1101/gad.274910.115.

Ogura, A., Inoue, K., and Wakayama, T. (2013). Recent advancements in cloning by somatic cell nuclear transfer. Philos. Trans. R. Soc. Lond. B Biol. Sci. *368*, 20110329. https://doi.org/10.1098/rstb.2011.0329.

Olins, A.L., and Olins, D.E. (1974). Spheroid chromatin units (ν bodies). Science *183*, 330–332.. https://doi.org/10.1126/science.183.4122.330.

Oliva, R. (2006). Protamines and male infertility. Hum. Reprod. Update *12*, 417–435.. https://doi.org/10.1093/humupd/dml009.

Ramachandran, S., and Henikoff, S. (2016). Transcriptional regulators compete with nucleosomes post-replication. Cell *165*, 580–592.. https://doi.org/10.1016/j.cell.2016.02.062.

Richmond, T.J., and Davey, C.A. (2003). The structure of DNA in the nucleosome core. Nature *423*, 145–150.. https://doi.org/10.1038/nature01595.

Segal, E., Fondufe-Mittendorf, Y., Chen, L., Thåström, A., Field, Y., Moore, I.K., Wang, J.P.Z., and Widom, J. (2006). A genomic code for nucleosome positioning. Nature *442*, 772–778.. https://doi.org/10.1038/nature04979.

Sekinger, E.A., Moqtaderi, Z., and Struhl, K. (2005). Intrinsic histone-DNA interactions and low nucleosome density are important for preferential accessibility of promoter regions in yeast. Mol. Cell *18*, 735–748.. https://doi.org/10.1016/j.molcel.2005.05.003.

Tachibana, M., Amato, P., Sparman, M., Gutierrez, N.M., Tippner-Hedges, R., Ma, H., Kang, E., Fulati, A., Lee, H.S., Sritanaudomchai, H., et al. (2013). Human embryonic stem cells derived by somatic

cell nuclear transfer. Cell *153*, 1228–1238.. https://doi.org/10.1016/j.cell.2013.05.006.

Tao, C., Li, J., Zhang, X., Chen, B., Chi, D., Zeng, Y., Niu, Y., Wang, C., Cheng, W., Wu, W., et al. (2017). Dynamic reorganization of nucleosome positioning in somatic cells after transfer into porcine enucleated oocytes. Stem Cell Rep. *9*, 642–653. https://doi.org/10.1016/j.stemcr.2017.06.004.

Tao, Y., Zheng, W., Jiang, Y., Ding, G., Hou, X., Tang, Y., Li, Y., Gao, S., Chang, G., Zhang, X., et al. (2014). Nucleosome organizations in induced pluripotent stem cells reprogrammed from somatic cells belonging to three different germ layers. BMC Biol. *12*, 109. https://doi.org/10.1186/s12915-014-0109-x.

Tessarz, P., and Kouzarides, T. (2014). Histone core modifications regulating nucleosome structure and dynamics. Nat. Rev. Mol. Cell Biol. *15*, 703–708. https://doi.org/10.1038/nrm3890.

Tolstorukov, M.Y., Sansam, C.G., Lu, P., Koellhoffer, E.C., Helming, K.C., Alver, B.H., Tillman, E.J., Evans, J.A., Wilson, B.G., Park, P.J., and Roberts, C.W.M. (2013). Swi/Snf chromatin remodeling/tumor suppressor complex establishes nucleosome occupancy at target promoters. Proc. Natl. Acad. Sci. U S A *110*, 10165–10170.. https://doi.org/10.1073/pnas.1302209110.

Van Thuan, N., Bui, H.T., Kim, J.H., Hikichi, T., Wakayama, S., Kishigami, S., Mizutani, E., and Wakayama, T. (2009). The histone deacetylase inhibitor scriptaid enhances nascent mRNA production and rescues full-term development in cloned inbred mice. Reproduction *138*, 309–317.. https://doi.org/10.1530/REP-08-0299.

Wakayama, S., Ohta, H., Hikichi, T., Mizutani, E., Iwaki, T., Kanagawa, O., and Wakayama, T. (2008). Production of healthy cloned mice from bodies frozen at −20°C for 16 years. Proc. Natl. Acad. Sci. U S A *105*, 17318–17322.. https://doi.org/10.1073/pnas.0806166105.

Wakayama, T., Perry, A.C.F., Zuccotti, M., Johnson, K.R., and Yanagimachi, R. (1998). Full-term development of mice from enucleated oocytes injected with cumulus cell nuclei. Nature *394*, 369–374.. https://doi.org/10.1038/28615.

Wakayama, T., Tabar, V., Rodriguez, I., Perry, A.C.F., Studer, L., and Mombaerts, P. (2001). Differentiation of embryonic stem cell lines generated from adult somatic cells by nuclear transfer. Science *292*, 740–743.. https://doi.org/10.1126/science.1059399.

Wang, C., Chen, C., Liu, X., Li, C., Wu, Q., Chen, X., Yang, L., Kou, X., Zhao, Y., Wang, H., et al. (2022). Dynamic nucleosome organization after fertilization reveals regulatory factors for mouse zygotic genome activation. Cell Res. https://doi.org/10.1038/s41422-022-00652-8.

Wang, L.Y., Li, Z.K., Wang, L.B., Liu, C., Sun, X.H., Feng, G.H., Wang, J.Q., Li, Y.F., Qiao, L.Y., Nie, H., et al. (2020). Overcoming intrinsic H3K27me3 imprinting barriers improves post-implantation development after somatic cell nuclear transfer. Cell Stem Cell *27*, 315–325.e5.. https://doi.org/10.1016/j.stem.2020.05.014.

Wen, D., Banaszynski, L.A., Liu, Y., Geng, F., Noh, K.M., Xiang, J., Elemento, O., Rosenwaks, Z., Allis, C.D., and Rafii, S. (2014). Histone variant H3.3 is an essential maternal factor for oocyte reprogramming. Proc. Natl. Acad. Sci. U S A *111*, 7325–7330.. https://doi.org/10.1073/pnas.1406389111.

Wilmut, I., Schnieke, A.E., McWhir, J., Kind, A.J., and Campbell, K.H.S. (1997). Viable offspring derived from fetal and adult mammalian cells. Nature *385*, 810–813.. https://doi.org/10.1038/385810a0.

Wu, J., Huang, B., Chen, H., Yin, Q., Liu, Y., Xiang, Y., Zhang, B., Liu, B., Wang, Q., Xia, W., et al. (2016). The landscape of accessible chromatin in mammalian preimplantation embryos. Nature *534*, 652–657.. https://doi.org/10.1038/nature18606.

Yamada, M., Johannesson, B., Sagi, I., Burnett, L.C., Kort, D.H., Prosser, R.W., Paull, D., Nestor, M.W., Freeby, M., Greenberg, E., et al. (2014). Human oocytes reprogram adult somatic nuclei of a type 1 diabetic to diploid pluripotent stem cells. Nature *510*, 533–536.. https://doi.org/10.1038/nature13287.

Yang, G., Zhang, L., Liu, W., Qiao, Z., Shen, S., Zhu, Q., Gao, R., Wang, M., Wang, M., Li, C., et al. (2021). Dux-mediated corrections of aberrant H3K9ac during 2-cell genome activation optimize efficiency of somatic cell nuclear transfer. Cell Stem Cell *28*, 150–163.e5.. https://doi.org/10.1016/j.stem.2020.09.006.

Yang, L., Liu, X., Song, L., Di, A., Su, G., Bai, C., Wei, Z., and Li, G. (2020). Transient Dux expression facilitates nuclear transfer and induced pluripotent stem cell reprogramming. EMBO Rep. *21*, e50054. https://doi.org/10.15252/embr.202050054.

Yang, X., Smith, S.L., Tian, X.C., Lewin, H.A., Renard, J.P., and Wakayama, T. (2007). Nuclear reprogramming of cloned embryos and its implications for therapeutic cloning. Nat. Genet. *39*, 295–302. https://doi.org/10.1038/ng1973.

Zaret, K.S., and Carroll, J.S. (2011). Pioneer transcription factors: establishing competence for gene expression. Genes Dev. *25*, 2227–2241. https://doi.org/10.1101/gad.176826.111.

Zhang, Y., Vastenhouw, N.L., Feng, J., Fu, K., Wang, C., Ge, Y., Pauli, A., van Hummelen, P., Schier, A.F., and Liu, X.S. (2014). Canonical nucleosome organization at promoters forms during genome activation. Genome Res. *24*, 260–266. https://doi.org/10.1101/gr.157750.113.

Zhu, F., Farnung, L., Kaasinen, E., Sahu, B., Yin, Y., Wei, B., Dodonova, S.O., Nitta, K.R., Morgunova, E., Taipale, M., et al. (2018). The interaction landscape between transcription factors and the nucleosome. Nature *562*, 76–81.. https://doi.org/10.1038/s41586-018-0549-5.